

MICROMETEORIC ABLATION BIPRODUCTS AS A HIGH ALTITUDE SOURCE FOR ICE NUCLEI IN THE PRESENT DAY MARTIAN ATMOSPHERE

V. L. Hartwick, *Department of Atmospheric and Ocean Sciences, Laboratory of Atmospheric and Space Physics, University of Colorado at Boulder, Boulder, CO, USA (vihal825@colorado.edu)*, **O. B. Toon**, *Department of Atmospheric and Ocean Sciences, Laboratory of Atmospheric and Space Physics, University of Colorado at Boulder, Boulder, CO, USA*

Introduction: High altitude water ice clouds have been observed on Mars since the mid-1980s and have been continuously monitored by orbiters for over 15 years (Jaquin 1986). High altitude clouds are observed year round with peak extinctions above 30-40 km and are distinct from lower altitude cloud and dust layers. Despite their prevalence, general circulation models struggle to replicate these observations. Clouds nucleate in atmospheric regions that are supersaturated with respect to water vapor and include a population of dust aerosols that can act as ice nuclei. In general, simulations restrict the source of ice nuclei to surface reservoirs and, for high altitude clouds, dust particles must then be lofted to altitudes far above the planetary boundary layer before nucleation can initiate. Such lofting is difficult. Without some additional forcing, such as intense vertical mixing within “rocket dust storms” (Spiga 2013), dust is largely confined within the lower 30 km of the atmosphere. Without a source of ice nuclei above this altitude, high altitude water ice clouds with the properties observed will not form in simulations.

On Earth, micrometeorite ablation byproducts act as ice nuclei for mesospheric noctilucent clouds in regions that are cold and aerosol depleted (Bardeen 2008, Flynn 1990). Conditions at the terrestrial polar summer mesopauses are similar to conditions at high altitudes on Mars. Observations with the Imaging Ultraviolet Spectrograph (IUVS) instrument on the Mars Atmosphere and Volatile Evolution (MAVEN) mission have observed persistent and transient ionized metallic layers consistent with year-round micrometeorite ablation (Schneider 2015, Crismani 2016). We therefore use a general circulation model to investigate the impact of including micrometeorites as a source of ice nuclei on cloud formation at high altitudes. Here, we present results from MarsCAM, a global climate model based on the U.S. National Center for Atmospheric Research Community Atmosphere Model, coupled with a physically based, state of the art cloud and dust microphysics model developed for Earth: the Community Aerosol and Radiation Model for Atmospheres (CARMA). We find that micrometeorites enhance cloud nucleation at high altitudes while also impacting the vertical distribution and size of ice cloud and dust particles at low altitudes. The radiative impact of aerosol layers

depends on the number of particles and particle size. High altitude water ice clouds, like lower altitude clouds, are sensitive to model parameterizations including: polar cap albedo, which impacts atmospheric water vapor; the atmospheric dust load, which impacts ice particle size; perturbations in the local atmospheric temperature, which impact supersaturation; and, the nucleation contact angle, which impacts the rate of formation of ice particles.

Methods: MarsCAM was first adapted to Mars from the terrestrial model CAM3.1 by Urata and Toon (2013). It has a finite volume dynamical core and conserves mass and ratios of advected tracers. I have coupled it with the University of Colorado/NASA CARMA model. Aerosols are treated within a bin-resolved sectional model and are allowed to advect, nucleate and sediment. Dust lifting is fully interactive and follows Kahre et al. (2006). Dust is lofted from reservoirs when surface wind stresses exceed 22.5 mN/m^2 . The total mass is initially distributed into a log-normal size distribution with a mode radius of $1.5 \text{ }\mu\text{m}$ and variance of 0.5. There are 40 dust size bins with bin center radii logarithmically distributed between 0.01 to $8.2 \text{ }\mu\text{m}$. Surface lofted dust is distributed only into bins with radii $0.1 \text{ }\mu\text{m}$ or larger.

The smallest dust bins are used to represent micrometeorite smoke particles. Observed micrometeorite ablation peaks at altitudes above the MarsCAM model top. As a first approximation, we therefore distribute a constant micrometeoritic mass evenly across the model top near 50-60km composed of monomodal spherical, $0.01 \text{ }\mu\text{m}$ radius particles. Total intercepted micrometeoroid mass is poorly constrained at Mars. Estimates range from 2900 to 59000 tons per year (Flynn 1990). MAVEN retrievals find a model derived micrometeoritic mass fluence of approximately 0.5 tons per day (Crismani 2016). We consider this value a lower limit. Here, we investigate the upper limit for intercepted micrometeoritic mass starting with a daily flux of 20 tons and assuming 100% ablation. We do not currently investigate the impact of seasonal or diurnal variability in micrometeoritic mass. We note that coagulation and cloud nucleation above the model top could conceivably impact both the dust particle size and number density.

Both surface and micrometeoritic dust are all owed

to act as sites for ice nucleation. MarsCAM – CARMA cloud microphysics include physically based parameterizations for nucleation, growth, evaporation and coagulation. To first order, nucleation rates depend on the contact parameter. We define a temperature dependent contact angle based on Trainer et al. (2009) with extreme values of 0.6 at 150K and 0.97 at 240K. High nucleation rates induce competition for limited atmospheric water vapor and, in general, cloud particles will be small with long lifetimes. By contrast, a low nucleation rate allows a few cloud particles to grow quickly to large sizes and sediment. The contact angle, ice nuclei population and atmospheric supersaturation are therefore important for, not only, the radiative impact of clouds, but also for the distribution and transport of clouds and water vapor. Water ice cloud bin center radii range from 0.014 to 118 μm . We choose the smallest ice bin radius such that dust and cloud bin particle masses are equal. Dust is carried inside the ice particles so that it can be released by evaporation.

Simulations: Common model parameters are summarized in Table 1. We discuss results from two simulations. Simulation A includes a ground source of dust only. Simulation B includes both surface dust lofted by wind and dust devils as well micrometeorite ablation bi-products.

Simulation	Micrometeoritic Dust
A	None
B	20 ton/day

Results: Dust number densities in simulations without micrometeorites fall off exponentially with altitude in all latitude bands (Figure 1, dashed lines). Numbers are negligible above 20 to 30 km. By contrast, simulations including micrometeorites (solid lines) have the highest number densities above 20 km and approach 10 particles per cubic centimeter for all latitudes at the model top. There is some variance with latitude that reflects large-scale circulation

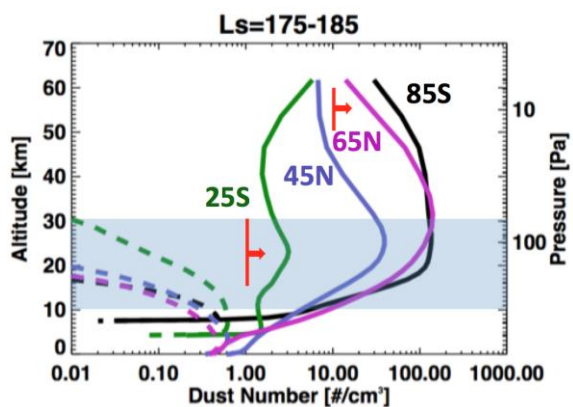


Figure 1: Zonal average dust number density $[\text{cm}^{-3}]$ versus altitude $[\text{km}]$ for Simulation A (dashed lines)

– ground source and Simulation B (solid line) – ground source + micrometeorites. Red lines mark the observational lower limits (Fedorova 2009).

patterns. The descending Hadley cell over the poles creates a deep layer of near constant number densities with altitude.

Data from the SPICAM on Mars Express (Spectroscopy for Investigation of Characteristics of the Atmosphere of Mars) has been used to constrain number density profiles versus altitude. However, SPICAM cannot observe all particle sizes with equal precision, and therefore observed particle numbers may represent a lower limit. Simulations without micrometeorites have number densities several orders of magnitude lower than observations at altitudes above 30km. Micrometeorites are necessary to simulate number densities equal to or greater than observations.

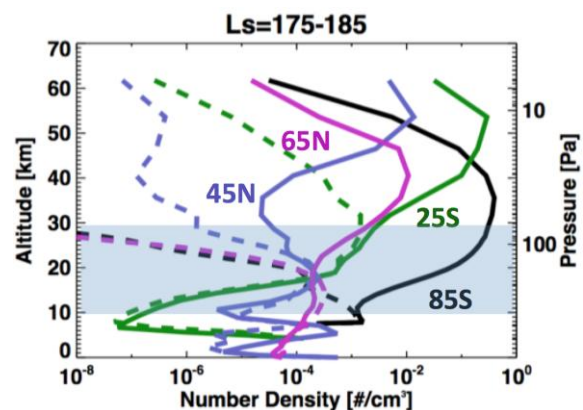


Figure 2: Zonal average ice number density $[\text{cm}^{-3}]$ versus altitude $[\text{km}]$ for Simulation A (dashed lines) – ground source and Simulation B (solid line) – ground source + micrometeorites.

Higher dust number densities translate to greater cloud particle number densities and 1.25 μm extinction at high altitudes. As shown in Fig. 2, at northern fall equinox ($L_s=180$), the aphelion cloud belt in the tropical atmosphere between 10 and 30 km altitude is dissipating. Mid-latitude high altitude clouds

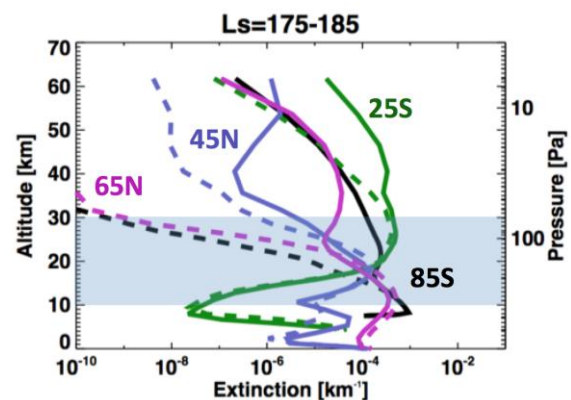


Figure 3: Zonal average ice extinction $[\text{km}^{-1}]$ versus altitude $[\text{km}]$ for Simulation A (dashed lines) – ground source and Simulation B (solid line) – ground source + micrometeorites.

altitude [km] for Simulation A (dashed lines) – ground source and Simulation B (solid line) – ground source + micrometeorites.

are common. Ice number densities are highest in the tropics and southern mid-latitudes above approximately 40 km. There is a secondary enhancement in ice number density corresponding to the aphelion cloud belt between 10 and 30 km. As in dust number densities, ice numbers between ~20 and 50 km are nearly constant with altitude over the southern pole. Simulations without micrometeorites show ice number densities with maxima in the low atmosphere capping dust layers.

Extinction depends on particle size, number and the wavelength dependent extinction coefficient. Although simulations with micrometeorites show a pronounced increase in particles numbers at high altitudes (Fig. 1 and 2) the responding change to extinction is not as developed (Fig. 3). However, secondary extinction maxima above 10-30 km are obvious, especially in the northern mid-latitudes at 45N and 65N. By comparison, ice extinctions in simulations with a ground source of ice nuclei only have latitude dependent maxima that cap dust layers and then fall off with altitude.

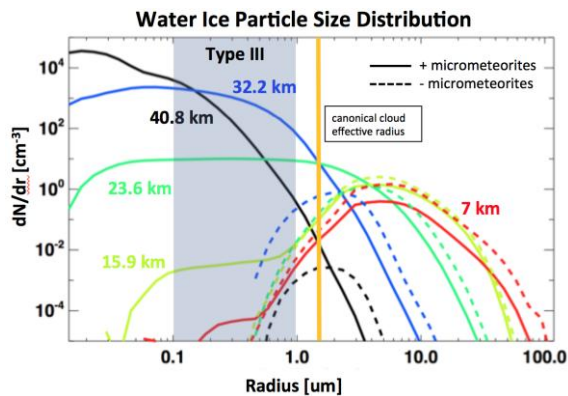


Figure 4: Equatorial (30S-30N) zonal average ice number [cm^{-3}] versus particle radius [μm] between $L_s=60-120$ for Simulation A (dashed lines) – ground source and Simulation B (solid line) – ground source + micrometeorites. The canonical cloud radius (1.5 μm) is marked by the vertical yellow line.

Particle size distributions reveal more detail about particle variation with altitude. Classically, particle size distributions follow log-normal or gamma distributions with mode radius near 1.5 μm . Simulations with a ground source of ice nuclei only (dashed lines) follow this distribution reasonably well. The addition of micrometeorites shifts ice nuclei and ice particle size distributions to smaller particle sizes (Fig. 4). Importantly, the size distribution varies with altitude. Above 30 km, the size distribution is dominated by submicron size ice particles. At 20 km, cloud particle numbers are nearly constant

over a broad range of particle sizes from less than 0.1 μm to almost 10 μm . Even at the lowest atmospheric levels, there is some low level enhancement in small particle sizes. Small particle sizes are consistent with sizes for type III aerosols identified in a number of observations (Montmessin 2006, Fedorova 2014, Clancy 2003)

The addition of micrometeorites as a secondary source of ice nuclei in the high martian atmosphere impacts the number densities of dust and cloud particles as well as the extinction. Simulations with micrometeorites reproduce high altitude cloud layers that are distinct from capping clouds at lower atmospheric levels. Cloud particle sizes above 30-40 km are small with sub-micron radii, consistent with observations of type III aerosol.

References: [1] C.G. Bardeen (2008) *J. Geophys. Res.* 113, D17202. [2] G.J. Flynn et al. (1990) *J. Geophys. Res.*, 95, 14497-14509. [3] R.T. Clancy et al. (2003) *J. Geophys. Res.*, 108, 5098. [4] Crismani, M. et al. (2016) *DPS 48/EPSC 11*, 16-21 October 2016, Pasadena, CA. [5] A.A. Fedorova et al. (2014) *Icarus* 231, 239-260. [6] F. Jaquin et al. (1986) *Icarus*, 68, 442-461. [7] M.A. Kahre et al. (2006) *J. Geophys. Res.* 111, E06008. [8] F. Montmessin et al. (2006) *J. Geophys. Res.*, 111, E09S09. [9] N. Schneider et al. (2015) *Geophys. Res. Lett.*, 42, 4755-4761. [10] A. Spiga et al. (2013) *J. Geophys. Res. Planets*, 118, 746-767. [11] M.G. Trainer et al. (2009) *J. Phys. Chem. C*, 113, 2036-2040. [12] R. Urata and O.B. Toon (2013) *Icarus*, 226(1), 336-354.